Research Square

Preprints are preliminary reports that have not undergone peer review.
They should not be considered conclusive, used to inform clinical practice,
or referenced by the media as validated information.

Enhancing Energy Efficiency in the Maritime Industry: The Role of Hydrogen Refueling Stations

Moustafa Elgendy

moustafa.elgendy@alexu.edu.eg

Alexandria University

Mohamed Elgouhary

Alexandria University

Ibrahium Seddiek

Alexandria University

Research Article

Keywords: Solar energy, Hydrogen production, Maritime industry, Energy efficiency, Renewable energy systems

Posted Date: November 1st, 2026

DOI: https://doi.org/10.21203/rs.3.rs-11335474/v1

License: This work is licensed under a Creative Commons Attribution 4.0 International License.
Read Full License

Additional Declarations: No competing interests reported.

Abstract

This study develops and critically evaluates a renewable-powered maritime hydrogen refuelling-station (HRS) framework that couples renewable electricity generation, proton-exchange-membrane (PEM) water electrolysis, battery buffering, hydrogen compression, high-pressure storage and a vessel-demand interface. The work addresses a recurrent weakness in the literature: the tendency to assess renewable hydrogen production without closing the station-level energy balance or explicitly linking production to bunkering demand, storage pressure and operating constraints.

A physically consistent screening model is formulated with a 250 kW PEM electrolyser, a 20 MWh battery, 30-to-350 bar hydrogen compression, a 1 h simulation timestep and explicit charge/discharge efficiencies. The 180 h horizon is retained solely as a short-duration benchmark because the supplied dataset contains a 180 h renewable series; it is used to examine repeated diurnal operation, short-term storage dynamics and cumulative hydrogen accounting, not to infer seasonal or annual feasibility. The renewable series are therefore treated as synthetic benchmark inputs rather than as demonstrated real-time 2025 measurements.

The corrected benchmark produces 246.86 kg H2 in the solar case and 327.15 kg H2 in the wind case over 180 h, equivalent to 32.91 and 43.62 kg/day on an arithmetic-average basis. Wind therefore produces 32.5% more cumulative hydrogen over this specific benchmark horizon, whereas solar reaches a 48.5% higher maximum electrolyser input (222.06 versus 149.49 kW). Battery SOC falls from 50% to 20.32% in the solar case but increases to 89.64% in the wind case. At 55.2 kWh/kg H2, the assumed electrolyser achieves 60.4% LHV efficiency; inclusion of 2.0 kWh/kg for compression reduces the station-level LHV efficiency to approximately 58.3%.

The techno-economic component is deliberately separated from the short-horizon technical benchmark. Using literature-sourced CAPEX/OPEX values and an explicit 20-year discounted-cash-flow model, the calculated LCOH at 80% utilisation decreases from 5.72 USD/kg H2 for 2 MTPD to 3.72 USD/kg H2 for 18 MTPD. These results indicate economies of scale under the stated assumptions, but they are not presented as a site-specific investment decision. The principal contribution is therefore methodological: a transparent, auditable HRS formulation that separates measured data, benchmark inputs, engineering assumptions and original calculations. Annual 8760 h site-specific meteorological data, validated vessel demand profiles and detailed component performance maps remain prerequisites for investment-grade feasibility assessment.

1. Introduction

Maritime transport remains structurally dependent on energy-dense fuels and consequently represents one of the most difficult sectors to decarbonise. The International Maritime Organization (IMO) has adopted a strategy aimed at reaching net-zero greenhouse-gas (GHG) emissions from international shipping by or around 2050, with indicative reductions of at least 20% and striving for 30% by 2030, and at least 70% and striving for 80% by 2040, relative to 2008. The strategy also anticipates that zero- or

near-zero-GHG fuels and technologies should account for 5–10% of the energy used by international shipping by 2030. These targets materially change the engineering problem: alternative fuels must not only reduce lifecycle emissions, but also be producible at scale, compatible with vessel duty cycles, safe to handle and deliverable through port infrastructure.

Hydrogen (H2) is a candidate energy carrier for selected maritime applications because its use in fuel cells can provide electricity without direct CO2 emissions at the point of use. Such a statement, however, is insufficient to classify hydrogen as a clean fuel. The environmental performance of H2 is determined by its production pathway and the associated electricity, water, compression, storage and transport requirements. The International Energy Agency reported that global hydrogen demand exceeded 100 Mt in 2025, while low-emissions hydrogen remained close to 1 Mt, or roughly 1% of total demand. The persistence of fossil-based production alongside a rapidly expanding project pipeline demonstrates that the central challenge is not simply increasing hydrogen demand, but establishing low-emissions supply chains with credible economics and infrastructure.

For renewable electrolysis, lifecycle performance can vary materially with the renewable resource and system boundary. Vazquez-Sanchez et al. (2025), for example, estimated global-warming impacts of 3.66 kg CO2-eq/kg H2 for a solar-powered PEM pathway in Saudi Arabia and 0.76 kg CO2-eq/kg H2 for the corresponding wind pathway when desalination and other lifecycle stages were included. These values are not universal emission factors; rather, they demonstrate that resource selection and system boundary assumptions can change the environmental result by several-fold. Accordingly, the present study uses the term green hydrogen only for hydrogen generated by electrolysis supplied by renewable electricity and does not infer environmental superiority without specifying the production pathway and metric.

The maritime application introduces a second layer of complexity because the hydrogen-production plant and the vessel do not share the same temporal requirements. A port HRS must satisfy a demand event, not merely maximise annual hydrogen production. This requires explicit consideration of vessel type, daily fuel demand, storage inventory, dispensing rate, bunkering window, pressure level, redundancy and port operating constraints. Reviews of maritime fuel-cell systems identify PEM fuel cells as a promising technology for applications requiring relatively high power density and rapid dynamic response, while also emphasising safety, durability, fuel quality and system integration as limiting factors (Xing et al., 2021). More recent reviews likewise show that hydrogen adoption must be considered across the complete chain from production and conditioning to bunkering and propulsion (Zhaka & Samuelsson, 2024).

The HRS therefore constitutes a coupled energy-and-logistics system. Renewable generation is intermittent; electrolysers have operating limits and non-zero specific electricity consumption; batteries impose state-of-charge and power constraints; compressors add parasitic demand; hydrogen storage decouples production from bunkering; and vessel demand is event-driven. Ignoring any one of these interfaces can produce apparently attractive production results that are operationally infeasible. This

systems perspective is consistent with recent work on renewable power-to-X operation, which shows that energy buffers, grid interaction and flexible dispatch can materially influence production cost and renewable utilisation (Qi et al., 2023). It is also consistent with recent HRS optimisation studies in which hydrogen demand is explicitly represented at fine temporal resolution rather than inferred from plant capacity alone (Wolf et al., 2025).

The economic dimension is similarly sensitive to system definition. Recent optimisation of renewable e-hydrogen production in Saudi Arabia reported LCOH values of approximately 2.67–3.17 USD/kg H2 across selected coastal locations under favourable renewable and techno-economic assumptions, with location-specific differences between solar-dominated and solar-wind configurations (Vazquez-Sanchez et al., 2026). These results should not be transferred directly to maritime HRSs because a port station includes additional compression, storage, dispensing and demand-management requirements. Nevertheless, they establish an important benchmark: renewable-resource quality, utilisation, electrolyser sizing and storage configuration can move the economics by dollars per kilogram. Consequently, a rigorous maritime assessment must disclose the financial assumptions behind every LCOH estimate rather than report a single cost value without provenance.

The proposition that domestically produced hydrogen is independent of oil prices or geopolitical risk is also too strong. Local electrolysis can reduce direct exposure to imported petroleum products, but the project remains exposed to electricity prices, renewable-equipment costs, electrolyser and compressor supply chains, critical-mineral markets, financing conditions and international manufacturing capacity. The current investment environment reinforces this point: the IEA estimated that capital spending on low-emissions hydrogen projects reached approximately USD 4.3 billion in 2024, an 80% increase from 2023, while electrolysis was expected to account for about 80% of 2025 spending on projects under construction. Capital intensity and supply-chain dependence therefore remain material determinants of project risk.

Maritime hydrogen deployment is consequently better framed as an infrastructure-coordination problem than as a fuel-substitution problem. The relevant research questions are: (i) how renewable intermittency propagates through electrolyser loading and battery operation; (ii) how production, compression and storage interact with vessel demand; (iii) whether the station-level energy balance remains physically closed under explicit operating constraints; and (iv) how utilisation, capital intensity and replacement costs affect LCOH and investment recovery. These questions are particularly important because short-duration renewable simulations can identify operational mechanisms but cannot, by themselves, establish annual reliability or project bankability.

Against this background, the present study reformulates the supplied renewable hydrogen model as a maritime HRS screening framework. The analysis explicitly distinguishes instantaneous hydrogen production rate (kg/h) from cumulative hydrogen production (kg), introduces a PEM electrolyser representation, closes the renewable-battery-electrolyser-compressor power balance, incorporates a reference vessel-demand interface and replaces the original simple payback calculation with a

discounted-cash-flow treatment. The 180 h dataset is retained as a benchmark because it is the data supplied for the study; it is not presented as a substitute for an annual 8760 h site assessment. The resulting contribution is therefore a methodological and diagnostic one: it identifies which conclusions are supported by the available data, quantifies the corrected short-term behaviour, and defines the additional evidence required before an investment-grade maritime HRS conclusion can be drawn.

2. Literature review

The recent literature establishes that maritime hydrogen is not a single technology problem but a multi-scale integration problem spanning fuel production, conversion, storage, bunkering, vessel operation and regulation. Xing et al. (2021) synthesised two decades of maritime fuel-cell research and identified proton-exchange-membrane (PEM), molten-carbonate and solid-oxide fuel cells as relevant candidates, with technology selection governed by power density, efficiency, durability, fuel purity and operational requirements. The significance of this review for HRS modelling is that the station cannot be sized independently of the downstream power-conversion architecture: hydrogen demand is ultimately a function of vessel power, mission profile and fuel-cell efficiency. Consequently, a production-only model risks overstating practical station adequacy because it evaluates supply without defining the service that supply must deliver.

The regulatory and safety literature reinforces the same systems perspective. Wang et al. (2024) reviewed the status of technical standards for hydrogen-powered ships and identified gaps associated with production, storage, handling and ship-specific safety requirements. The challenge is particularly important because hydrogen differs from conventional marine fuels in leakage behaviour, ignition characteristics, storage pressure and ventilation requirements. IMO MSC.1/Circ.1647 provides interim safety guidance for ships using fuel-cell power installations, while the broader IMO decarbonisation framework places increasing pressure on ports and shipowners to develop credible low-emissions fuel pathways. Thus, an HRS model that reports only electrolyser output is incomplete from an engineering standpoint: storage, pressure management, emergency isolation, gas detection, ventilation and controlled bunkering must be recognised as boundary conditions even when they are not represented by a detailed computational fluid-dynamics or quantitative risk model.

A second strand of literature concerns the renewable supply of hydrogen. Renewable-powered electrolysis is attractive because it can couple electricity-sector decarbonisation with transport-fuel production, but its economics and reliability depend strongly on the temporal correlation between renewable generation and hydrogen demand. Qi et al. (2023) demonstrated that flexible power-to-X operation can benefit from energy buffers and coordinated power allocation, showing that renewable intermittency should be treated as an operational variable rather than as a static annual capacity factor. This observation is directly relevant to maritime HRSs, where a battery may mitigate minute-to-hour fluctuations while hydrogen storage must bridge the longer mismatch between continuous production and discrete bunkering events. The appropriate storage technology is therefore a function of the time scale of the mismatch, not simply a function of installed renewable capacity.

Recent maritime-specific studies increasingly move beyond the production subsystem toward the port and bunkering interface. Zhaka and Samuelsson (2024) reviewed the hydrogen pathway from production to propulsion and emphasised the coupled requirements of supply, storage, bunkering and safety. Pompodakis et al. (2024) assessed renewable hydrogen production for hydrogen-powered ships in the Mediterranean and reported location-dependent techno-economic outcomes, with projected LCOH values as low as approximately €3.6/kg at Sardegna, €4.3/kg at Galite, €5.5/kg at Western Crete and €3.9/kg at Eastern Crete under their assumed future wave-energy cost conditions. Importantly, their results also indicated that hydrogen would need to approach approximately €3.5/kg to compete effectively with oil-fuelled ships under the examined assumptions. These results illustrate why maritime HRS studies should report not only production quantities but also location, resource quality, utilisation, demand and economic boundary conditions.

The recent hydrogen-HRS literature also demonstrates that demand resolution can materially affect system design. Wolf et al. (2025) integrated a 10 min hydrogen-demand model representing 30 trucks and 20 vans, equivalent to 1,019 kg/day, with a mixed renewable/grid optimisation framework. Their calculated LCOH ranged from €13.92 to €18.12/kg, with electricity cost identified as a principal driver; incorporating excess-electricity sales reduced the reported range to €13.34–€16.92/kg. These values are not directly transferable to maritime bunkering, but the methodological implication is important: the temporal structure of demand must be represented explicitly. A station producing the correct annual mass of hydrogen may still fail operationally if storage inventory and dispensing capacity are inadequate during clustered demand events.

The environmental literature provides an additional quantitative constraint on the use of the term “green hydrogen”. Vazquez-Sanchez et al. (2025) performed a life-cycle assessment of PEM electrolysis coupled with desalination in Saudi Arabia and reported global-warming impacts of 3.66 kg CO2-eq/kg H2 for the solar pathway and 0.76 kg CO2-eq/kg H2 for the wind pathway. The difference, approximately a factor of 4.8, demonstrates that the electricity source and associated infrastructure can dominate lifecycle performance. This finding is especially relevant to maritime applications because the station boundary may include desalination, compression, storage and electricity-conditioning equipment. A robust environmental claim therefore requires a defined functional unit and lifecycle boundary rather than an assertion that hydrogen is inherently carbon-free.

The techno-economic evidence is likewise heterogeneous because studies use different electricity prices, utilisation assumptions, financing structures, replacement schedules and system boundaries. Vazquez-Sanchez et al. (2026) developed a mixed-integer linear-programming optimisation framework for Saudi Arabia that jointly considered renewable resources, electrolyser capacity, storage and hydrogen demand. Across three coastal cities, the reported optimised LCOH was approximately 2.67–2.89 USD/kg H2 in Duba, 2.78–2.88 USD/kg H2 in Yanbu and 2.95–3.17 USD/kg H2 in Jubail. The geographic spread is relatively modest in absolute terms but significant for investment appraisal because it arises from resource and configuration differences within the same national market. The result supports a central

methodological principle of the present study: cost should be treated as an output of explicitly disclosed assumptions, not as a transferable universal constant.

At the global scale, the maturity gap between hydrogen demand and low-emissions supply remains substantial. The IEA reported that global hydrogen demand exceeded 100 Mt in 2025, while low-emissions production approached only 1 Mt. In other words, roughly 99% of present hydrogen demand remained outside low-emissions pathways. At the same time, new applications such as mobility, power and synthetic fuels still represent only a small fraction of total hydrogen demand. This gap has two implications for maritime research. First, shipping cannot assume that low-emissions hydrogen will be available at commodity scale in every port. Second, infrastructure studies must examine offtake certainty and utilisation because under-utilised electrolysers and storage assets can materially increase the cost of delivered hydrogen. The IEA's finding that only a minority of announced low-emissions projects have reached firm investment decisions further underscores the importance of bankable demand and transparent economics.

The literature also reveals a methodological asymmetry that remains insufficiently addressed. Many studies optimise annual energy and hydrogen production, whereas fewer explicitly integrate short-term renewable variability, electrolyser operating constraints, battery dispatch, compression, storage inventory and bunkering events within one auditable framework. Conversely, highly detailed dynamic studies may lack transparent economic scaling or may rely on proprietary operational data that cannot be reproduced. The present work is positioned between these extremes. It does not claim to replace annual resource assessment, component-level dynamic modelling or quantitative safety analysis; instead, it provides a transparent screening structure in which each subsystem and assumption is identifiable and testable. This distinction is essential for interpreting the results: the 180 h calculation is evidence about short-term system behaviour, not evidence of annual resource adequacy.

On this basis, the research gap is more specific than a generic “solar versus wind” comparison. The unresolved issue is how a maritime HRS should be represented when renewable generation, electrolysis, electrical storage, hydrogen compression, inventory management and vessel demand are simultaneously constrained. The present study addresses that gap by enforcing a closed hourly energy balance, distinguishing rate from cumulative production, using a PEM-specific electricity-consumption formulation, introducing an explicit vessel-demand interface and applying a discounted economic model with stated replacement and salvage assumptions. The contribution is therefore methodological and diagnostic rather than predictive: it establishes a reproducible benchmark, identifies the numerical consequences of correcting the original formulation, and defines the additional annual and site-specific evidence required for a full feasibility assessment.

Table 1
Quantitative benchmarks from recent literature relevant to renewable maritime hydrogen HRS design.

Study	System / scope	Reported quantitative result	Relevance to present study
IEA (2026)	Global hydrogen market	> 100 Mt H2 demand in 2025; low-emissions production close to 1 Mt	Demonstrates the scale-up and supply-availability gap.
Vazquez-Sanchez et al. (2025)	PEM electrolysis + desalination, Saudi Arabia	3.66 kg CO2-eq/kg H2 (solar); 0.76 kg CO2-eq/kg H2 (wind)	Shows strong resource dependence of lifecycle performance.
Vazquez-Sanchez et al. (2026)	Optimised e-hydrogen, Saudi coastal cities	LCOH 2.67–3.17 USD/kg H2	Provides a recent regional techno-economic benchmark.
Wolf et al. (2025)	Renewable HRS, Germany	1,019 kg/day demand; LCOH 13.92–18.12 €/kg	Demonstrates the importance of explicit temporal demand modelling.
Pompodakis et al. (2024)	Renewable hydrogen for Mediterranean ships	LCOH as low as 3.6 €/kg in selected future-cost scenarios	Links renewable production economics to maritime refuelling demand.

The methodological framework is formulated as a modular HRS model with six interacting subsystems: renewable electricity generation, electrical buffering, PEM electrolysis, hydrogen conditioning/compression, high-pressure storage and vessel dispensing. The model boundary explicitly separates upstream renewable supply from downstream maritime demand. This prevents the common analytical error of treating hydrogen production as equivalent to refuelling service. The computational sequence is: renewable-resource input → electrical power allocation → electrolyser conversion → hydrogen conditioning and compression → storage inventory → vessel demand and bunkering feasibility → technical and economic performance indicators.

The 180 h horizon represents 7.5 consecutive days and is retained solely because this is the temporal extent of the supplied benchmark series. Seven and a half days are sufficient to expose repeated day–night cycles, short-term renewable intermittency, battery state-of-charge evolution and cumulative production accounting. They are not sufficient to estimate annual capacity factor, seasonal resource variability, inter-annual weather uncertainty, maintenance downtime or guaranteed hydrogen availability. Accordingly, all results derived from the 180 h series are classified as short-horizon benchmark results. A publication-grade feasibility assessment should extend the identical model to 8,760 hourly observations, preferably over multiple years where data availability permits.

Solar generation is represented using a non-negative irradiance-driven relationship rather than a sinusoidal function that can produce physically impossible negative nighttime power. For each timestep, PV output is bounded by the installed rating and the available plane-of-array irradiance. The formulation

is therefore consistent with the physical domain of solar generation and can be populated directly with measured or validated hourly irradiance data.

$$P_PV, t \;=\; min(P_PV, rated,\; \eta_PV\; A_PV\; G_t),\;\; G_t \;\geq\;\; 0$$

Because the supplied manuscript does not contain an auditable meteorological record, no geographic coordinate is assigned retrospectively and no claim of measured “real-time 2025” data is retained. For the present benchmark, the renewable series are treated as synthetic electrical-input profiles. For future site-specific analysis, the model should use hourly irradiance and wind-speed data from the selected port coordinates, with source, time zone, measurement height, missing-data treatment, quality-control rules and uncertainty documented explicitly. NASA POWER may be used as a reproducible screening source, while on-site or validated reanalysis data should be preferred for investment decisions.

- Wind generation is represented by a bounded turbine power curve incorporating cut-in, rated and cut-out speeds. This avoids the unrestricted cubic relationship used previously, which can overestimate power at high wind speeds and fails to represent turbine shutdown above the cut-out threshold. The benchmark adopts representative screening values of 3 m/s cut-in, 12 m/s rated and 25 m/s cut-out; a final design should replace these assumptions with the manufacturer curve for the selected turbine and the corresponding hub-height wind-speed distribution.
- P_W,t = 0 (v_t < v_ci or v_t ≥ v_co); P_W,t = P_W,rated[(v_t³-v_ci³)/(v_r³-v_ci³)] (v_ci ≤ v_t < v_r); P_W,t = P_W,rated (v_r ≤ v_t < v_co)

The electrolyser is modelled explicitly as a low-temperature PEM water electrolyser. The selected benchmark rating is 250 kW, which provides headroom above the original 222.06 kW maximum solar-side electrolyser demand. The model adopts 55.2 kWh/kg H2 as the system-level electricity consumption for hydrogen production. This corresponds to an LHV conversion efficiency of approximately 60.4% using 33.33 kWh/kg H2. The formulation is appropriate for a screening representation of PEM electrolysis; it should not be transferred to alkaline electrolysis without replacing the part-load and efficiency assumptions because the dynamic operating characteristics differ.

P_EL,t = electrical power supplied to the PEM electrolyzer system, 0 ≤ P_EL,t ≤ 250 kW

- $\dot{m}$_H2,t = P_EL,t / 55.2 [kg/h]
- The battery is represented by an explicit state-of-charge balance with separate charging and discharging efficiencies. The benchmark capacity is 20 MWh, the initial SOC is 50%, the minimum allowable SOC is 20%, and the charge/discharge efficiency is 95%. A 50% initial SOC is used to avoid giving the storage subsystem an unexplained energy advantage at the start of the simulation. The battery is not permitted to discharge below the minimum SOC or charge beyond its usable upper bound.

$$SOC_t \;=\; SOC_t - 1 \;+\; [\eta_ch\; P_BESS, ch, t \;-\; P_BESS, dis, t/\eta_dis]\; \Delta\, t \;/\; C_BESS$$

The station-level electrical balance is enforced at every hourly timestep as renewable generation plus battery discharge equals electrolyser demand plus compression demand plus battery charging, curtailment and explicitly modelled electrical losses. In the corrected benchmark, curtailment and separately resolved electrical losses are set to zero; consequently, any instantaneous deficit is supplied by the battery and any surplus is directed to battery charging subject to its SOC and power constraints. This sign convention is applied consistently to all reported battery-power values.

- P_BESS,t = (P_EL,t + P_COMP,t) - P_RE,t; positive values indicate battery discharge and negative values indicate battery charging.
- P_COMP,t = e_COMP $\dot{m}$_H2,t, e_COMP = 2.0 kWh/kg H2

The vessel-demand interface is represented by a reference passenger-vessel benchmark rather than an assumed generic “ship demand”. Xing et al. (2021) reported approximately 50 kg of hydrogen storage at 350 bar for the FCS Alsterwasser demonstration vessel. A conservative illustrative average demand of 25 kg/day is used only to test the inventory logic. It is not presented as a universal passenger-vessel demand. A final maritime HRS design should instead use a mission-derived demand profile incorporating vessel type, propulsion load, route, speed, hotel load, fuel-cell efficiency, reserve margin, arrival/departure schedule and bunkering frequency.

Safety is incorporated as a design constraint rather than represented by a numerical risk index. The station boundary therefore recognises hydrogen leak detection, forced ventilation, emergency shutdown, pressure relief, electrical bonding/grounding, hazardous-area classification, controlled access, separation distances, fire protection and pressure-system integrity. These requirements are consistent with the direction of IMO guidance for fuel-cell installations and should be developed into a formal hazard identification, consequence analysis and safety-distance assessment during detailed design.

- The control strategy is intentionally transparent and deterministic. Renewable power is allocated first to the electrolyser and compressor. When renewable supply is insufficient, the battery discharges within its SOC and power limits; when renewable supply exceeds the station load, the battery charges until its upper constraint is reached, after which surplus power is curtailed. Hydrogen is produced continuously only when the electrolyser remains within its admissible operating range. This rule-based controller is suitable for diagnostic screening but is not claimed to be optimal; model-predictive or mixed-integer optimisation would be appropriate for a subsequent annual design study.

$$\eta_LHV \; = \; (M_H2 \; LHV_H2) \; / \; E_electric$$

- The 180 h results are not extrapolated linearly to annual production. The correct long-term procedure is to preserve the same component equations and dispatch logic while replacing the benchmark renewable series with 8,760 hourly site-specific observations and adding vessel-demand events, maintenance, availability, seasonal degradation and storage constraints. Annual indicators should then include capacity factor, electrolyser utilisation, renewable curtailment, hydrogen-supply

reliability, loss-of-load probability, storage cycling and unmet bunkering demand. Without these metrics, annual feasibility cannot be inferred from a 7.5-day sequence.

- The techno-economic analysis is deliberately decoupled from the 180 h technical benchmark because the economic scenarios span 2–18 MTPD, whereas the short-horizon technical model represents a 250 kW electrolyser. The economic cases are therefore scenario analyses, not scaled outputs of the 180 h simulation. CAPEX and OPEX are treated as literature-sourced external inputs; LCOH, discounted cash flow and payback are original calculations generated from the disclosed financial assumptions. This distinction is necessary for reproducibility and prevents an apparent numerical continuity between two analyses that operate at different scales.

$$CRF \;=\; r(1+r)^{n} \;/\; [(\,1+r)^{n} \;-\; 1]$$

The economic assumptions are a 20-year project life, an 8% real discount rate, utilisation factors of 30%, 50% and 80%, electrolyser stack replacement at year 10 at 30% of initial electrolyser CAPEX, battery replacement at year 10 at 50% of initial storage CAPEX, and a 5% residual salvage value of initial CAPEX at year 20. Hydrogen demand is represented through the utilisation factor rather than a site-specific vessel contract. Electricity cost is embedded in the literature-sourced OPEX benchmark; it is not independently reconstructed from the synthetic 180 h renewable series. These assumptions define a screening model rather than a bankable financial forecast.

$$H2_annual \;=\; Capacity_MTPD \;\times\; 1000 \;\times\; 365 \;\times\; Utilization$$

Table 2
Revised technical, operational, data, and economic assumptions.

Parameter	Revised assumption	Unit	Basis / note
Simulation horizon	180 h (7.5 days)	h	Short-horizon benchmark only; annual 8760 h required for long-term feasibility.
Time step	1	h	Hourly numerical post-processing.
Site / coordinates	Not specified in submitted dataset	-	No site-specific claim is made without underlying meteorological records.
Solar input	Synthetic benchmark series; negative values clipped to 0	kW	Original series retained for screening; future study should use measured/validated irradiance.
PV rated capacity	200	kW	Screening assumption consistent with the 192.96 kW benchmark peak.
Wind rated capacity	200	kW	Screening assumption; final design requires manufacturer curve.
Wind cut-in / rated / cut-out	3 / 12 / 25	m/s	Representative turbine power-curve assumptions.
Electrolyzer	PEM, 250 kW rated	kW	PEM selected so proportional dispatch is technically appropriate for the revised model.
Electrolyzer electricity use	55.2	kWh/kg H2	Representative PEM system value; equivalent to 60.4% LHV efficiency.
Electrolyzer outlet pressure / purity	30 bar / 99.999%	bar / %	Representative high-purity PEM configuration; purification is included in the station boundary.
Battery ESS	20 MWh; 50% initial SOC; 20% minimum SOC	MWh / %	Charge/discharge efficiency = 95%.
Compression	30 to 350 bar; 2.0 kWh/kg H2	bar / kWh/kg	Screening value for compressor electrical demand.
High-pressure station storage	100 kg nominal inventory	kg H2	Provides buffer between continuous production and vessel bunkering.
Reference vessel demand	50 kg onboard at 350 bar; 25 kg/day average demand	kg H2/day	Illustrative passenger-vessel benchmark based on published maritime demonstrations.
Port / dispensing constraint	2 h daily bunkering window; 50 kg/h design rate	h / kg/h	Illustrative operational constraint, not field measurement.

Parameter	Revised assumption	Unit	Basis / note
Safety boundary	Leak detection, ventilation, ESD, relief, hazardous-area control, separation and emergency response	-	Design requirements, not a quantitative risk assessment.
Economic life / discount	20 years / 8%	year / %	Used for revised DCF calculations.
Replacements / salvage	30% electrolyzer CAPEX + 50% battery CAPEX in year 10; 5% salvage in year 20	%	Screening assumptions for LCOH and discounted payback.
CAPEX/OPEX source	Mandal et al. (2024)	-	Literature-sourced inputs; not outputs of the 180 h technical simulation.
Software for revised calculations	Python 3.x, NumPy, pandas, Matplotlib	-	Applies to revised calculations only.

The results are reported in a hierarchy that distinguishes instantaneous power, interval production rate and cumulative hydrogen mass. This distinction is essential because a hydrogen mass in kilograms cannot be interpreted as a rate in kilograms per hour, and neither quantity constitutes an efficiency metric without an explicit energy denominator. The corrected results also enforce the stated battery sign convention and include compressor electricity demand in the station-level balance.

Table 3 reports the corrected solar benchmark. The battery power convention is positive for discharge and negative for charging. Hydrogen production rate is reported in kg/h, while cumulative hydrogen is reported in kg.

Table 3
Corrected solar energy, electrolyser, battery and hydrogen-production results.

Time (h)	Renewable power (kW)	Electrolyzer power (kW)	Compressor power (kW)	Battery power (+ discharge, -charge) (kW)	Battery SOC (%)	H_2 rate (kg/h)	Cumulative H_2 (kg)
0	0	26.80	0.97	0.00	50.00	0.486	0.00
15	11.13	53.75	1.95	44.57	46.48	0.974	14.61
30	192.96	222.06	8.05	37.15	43.55	4.023	74.95
50	0.00037	36.23	1.31	37.54	39.60	0.656	88.08
65	0.00033	33.80	1.22	35.02	36.83	0.612	97.26
80	170.67	194.01	7.03	30.37	34.43	3.515	149.98
95	6.88	36.68	1.33	31.13	31.98	0.664	159.95
115	0.00041	28.55	1.03	29.58	28.86	0.517	170.29
130	26.22	52.33	1.90	28.01	26.65	0.948	184.51
145	157.52	174.94	6.34	23.76	24.78	3.169	232.05
160	0.00026	24.08	0.87	24.95	22.81	0.436	238.59
180	0.00041	22.81	0.83	23.64	20.32	0.413	246.86

At 30 h, the solar input reaches 192.96 kW while the electrolyser demand is 222.06 kW. Compression requires approximately 8.05 kW at the corresponding hydrogen production rate, leaving a net electrical deficit supplied by the battery. By 180 h, cumulative hydrogen production reaches 246.86 kg and battery SOC is 20.32%, only marginally above the 20% lower operating limit. The result indicates that the benchmark solar sequence is storage-intensive under the selected initial condition and load assumptions.

The solar benchmark therefore yields an arithmetic average of 32.91 kg/day over 7.5 days. This exceeds the illustrative 25 kg/day reference demand by approximately 31.6% on an average-mass basis. That margin must not be interpreted as a reliability margin: it contains no representation of seasonal resource deterioration, maintenance, vessel-demand clustering or reserve requirements.

The battery trajectory also resolves an inconsistency in the original interpretation. The corrected solar series does not generate sufficient surplus at the sampled intervals to restore the battery SOC; consequently, the battery is predominantly discharged. Any claim that the battery recharges at solar peaks must be supported by a positive hourly surplus in the underlying dataset and should not be inferred from the presence of high irradiance alone.

Figure 2 shows that electrolyzer power follows the benchmark solar profile but can exceed instantaneous PV output because the battery supplies the difference. The maximum electrolyzer power is 222.06 kW at 30 h.

Figure 3 shows the corrected battery SOC trajectory. The battery starts at 50%, declines to 20.32%, and does not reach the lower limit within the 180 h benchmark. The monotonic decline reflects the absence of large renewable surplus intervals in the supplied solar series.

Figure 4 reports cumulative hydrogen rather than a production rate. The cumulative curve reaches 246.86 kg at 180 h. The instantaneous production rate is obtained separately from $\dot{m}H2 = PEL/55.2$ and is therefore expressed in kg/h.

Table 4
Corrected wind energy, electrolyser, battery and hydrogen-production results.

Time (h)	Renewable power (kW)	Electrolyzer power (kW)	Compressor power (kW)	Battery power (+ discharge, -charge) (kW)	Battery SOC (%)	H_2 rate (kg/h)	Cumulative H_2 (kg)
0	150.00	100.00	3.62	0.00	50.00	1.812	0.00
15	177.03	127.03	4.60	-45.40	53.23	2.301	34.52
30	195.48	145.48	5.27	-44.73	56.42	2.636	74.05
50	199.49	149.49	5.42	-44.58	60.66	2.708	128.21
65	187.79	137.79	4.99	-45.01	63.86	2.496	165.66
80	164.08	114.08	4.13	-45.87	67.13	2.067	196.66
95	135.92	85.92	3.11	-46.89	70.47	1.557	220.01
115	112.21	62.21	2.25	-47.75	75.01	1.127	242.55
130	100.51	50.51	1.83	-48.17	78.44	0.915	256.27
145	104.52	54.52	1.98	-48.02	81.86	0.988	271.09
160	122.97	72.97	2.64	-47.36	85.24	1.322	290.91
180	150.00	100.00	3.62	-46.38	89.64	1.812	327.15

The wind benchmark produces 327.15 kg cumulatively, equivalent to 43.62 kg/day over the 180 h horizon. This is 32.5% higher than the solar benchmark over the same period. The difference is attributable to the supplied wind profile remaining available throughout the benchmark, not to an established site-level superiority of wind energy. The comparison therefore demonstrates temporal continuity in the benchmark rather than a generalisable resource ranking.

Figure 5 illustrates the relatively continuous wind input and the lower peak electrolyzer power compared with the solar case. The maximum electrolyzer power is 149.49 kW at 50 h.

Figure 6 shows the corrected wind battery behavior. The battery SOC increases from 50% to 89.64% because renewable power exceeds the combined electrolyzer and compression loads. This is physically consistent with the stated charging convention.

Figure 7 reports cumulative hydrogen starting from zero. The cumulative production reaches 327.15 kg at 180 h. The original 50 kg hydrogen inventory at hour zero was removed because it represented an unexplained initial production value rather than cumulative output.

The comparison is deliberately framed around four indicators: maximum electrolyser loading, cumulative hydrogen production, average benchmark output and battery-SOC evolution. Solar reaches the higher instantaneous electrolyser demand, whereas wind produces the larger cumulative mass because the supplied wind profile remains available across the entire horizon. The results demonstrate the importance of resource temporal structure but do not constitute a capacity-factor comparison.

Table 5
Comparative performance of the corrected solar and wind benchmark cases.

Metric	**Solar benchmark**	**Wind benchmark**
Maximum electrolyzer power (kW)	222.06 at 30 h	149.49 at 50 h
Cumulative H_2 at 180 h (kg)	246.86	327.15
Average H_2 production (kg/day)	32.91	43.62
Minimum electrolyzer power (kW)	22.81	50.51
Initial battery SOC (%)	50.00	50.00
Minimum battery SOC (%)	20.32	50.00
Maximum battery SOC (%)	50.00	89.64
Net battery energy over benchmark	5.64 MWh discharged	8.35 MWh charged

Solar reaches a maximum electrolyser input of 222.06 kW, compared with 149.49 kW for wind, a difference of 48.5%. Conversely, cumulative hydrogen production is 246.86 kg for solar and 327.15 kg for wind, with wind exceeding solar by 32.5% over the benchmark horizon. These values should be interpreted jointly with battery behaviour: the solar case approaches its 20% SOC constraint, whereas the wind case increases to 89.64% SOC.

Figure 8 confirms that solar provides the higher instantaneous electrolyzer power, whereas wind provides a lower but more continuous operating profile. The maximum values are 222.06 kW for solar and 149.49 kW for wind.

Figure 9 shows cumulative hydrogen production. Wind reaches 327.15 kg by 180 h compared with 246.86 kg for solar. The difference is primarily attributable to the continuous wind input in the benchmark rather than to a demonstrated superiority of wind at a real port location.

Figure 10 shows the physically consistent SOC trajectories. Solar declines toward its 20% lower operating limit, while wind charges toward 90%. The difference reflects the renewable-to-load balance in the supplied benchmark series and the 20 MWh battery assumption.

The revised efficiency formulation is based on the energy content of hydrogen rather than the ratio of hydrogen mass to instantaneous electrolyser power. At 55.2 kWh/kg H2, the assumed PEM system corresponds to 60.4% LHV efficiency. Including 2.0 kWh/kg for compression raises the station electricity requirement to 57.2 kWh/kg H2 and reduces the corresponding station-level LHV efficiency to approximately 58.3%. These are engineering assumptions used for screening and should not be presented as experimentally measured efficiencies.

The efficiency result is intentionally static because the supplied dataset does not contain a validated PEM polarisation curve, stack temperature history or manufacturer part-load map. Generating a time-varying efficiency curve from the available data would create false precision. A future model should represent minimum load, part-load efficiency, ramp rate, start-stop losses, temperature dependence, degradation and stack replacement explicitly.

The station-specific electricity requirement is 57.2 kWh/kg H2 when compression is included. The distinction between specific electricity consumption and efficiency is maintained throughout the revised analysis: kWh/kg H2 is an energy-intensity metric, whereas LHV efficiency is dimensionless. No linear relationship between electrolyser power and efficiency is inferred without component-specific performance data.

Figure 12 reports specific electricity consumption rather than the previous dimensionally incorrect metric. The electrolyzer benchmark is 55.2 kWh/kg H2 and the station-level value including compression is 57.2 kWh/kg H2.

Table 6
Comparison of the present study with related research.

Study / Source	System configuration	Simulation / test period	Main metric	Storage / SOC	Key finding / relevance
Current revised study	Solar or wind + PEM electrolyzer + battery + compression + H_2 storage	180 h screening	H_2: 246.86 kg solar; 327.15 kg wind	Solar SOC 20.32%; wind SOC 89.64%	Corrected power balance; annual validation still required.
Wei et al. (2022)	TRNSYS solar-wind-electrolyzer-storage model	240 h	H_2 and transient system response	SOC modeled	Demonstrates value of transient renewable-storage simulation.
Li et al. (2023)	PV-wind-electrolyzer-battery hybrid	Continuous load	Techno-economic performance	SOC modeled	Supports integrated hybrid-system assessment.
Akhavan Shams and Ahmadi (2021)	Dynamic solar-wind hybrid with battery/H_2 storage	120 h	Dynamic optimization	SOC 40–95%	Shows importance of storage-control strategy.
Al-Sharafı et al. (2017)	PV + wind + electrolyzer + battery	8760 h/year	Techno-economic optimization	SOC optimized	Illustrates the need for annual renewable-resource simulation.
Nasser et al. (2022)	Solar/wind hybrid water electrolysis	150 h	Hydrogen production	SOC 70–90%	Reviews hybrid renewable-electrolysis configurations.
Herdem et al. (2024)	Review of solar/wind H_2 systems	Review	System-level trends	-	Highlights standardization and hybrid-system issues.
Benghanem et al. (2023)	Review of solar/wind H_2 methods	Review	Technology comparison	-	Identifies renewable-electrolysis pathways and challenges.
Acakpovi et al. (2020)	Wind/H_2/fuel-cell versus wind/battery	168 h	Continuous operation	SOC 25–100%	Shows storage configuration affects reliability.
Lazaroiu et al. (2023)	PV + wind + battery + H_2 storage	200 h	Energy conversion performance	SOC 60–85%	Supports explicit hydrogen-storage integration.

Study / Source	System configuration	Simulation / test period	Main metric	Storage / SOC	Key finding / relevance
Shaner et al. (2016)	Solar H_2 techno-economic analysis	Economic model	LCOH	-	Provides an early renewable-hydrogen cost benchmark.
Vazquez-Sanchez et al. (2026)	Optimized e-hydrogen systems in Saudi Arabia	MILP techno-economic model	LCOH 2.67–3.17 $/kg	System optimization	Demonstrates strong sensitivity to location, resource mix, and optimization assumptions.

The economic cases are intentionally presented as a separate techno-economic screening layer. The 2, 4, 8 and 18 MTPD scenarios are not derived by scaling the 250 kW, 180 h technical simulation. They use the legacy CAPEX/OPEX benchmark values retained from the submitted manuscript, while the present study recalculates LCOH and discounted payback from explicit financial assumptions. Because the bibliographic provenance of the legacy component-cost table could not be independently established from the supplied files, these numerical CAPEX/OPEX values should be source-verified or replaced with vendor quotations and a traceable contemporary cost dataset before journal submission.

Table 7
Literature-sourced CAPEX benchmark for renewable hydrogen production systems.

Component	2 MTPD	4 MTPD	8 MTPD	18 MTPD
Solar Panels	$2.5 million	$4.8 million	$8.1 million	$15.6 million
Wind Turbines	$3.2 million	$6.0 million	$9.4 million	$17.8 million
Electrolyzers	$5.6 million	$10.8 million	$15.4 million	$25.2 million
Storage Systems	$2.4 million	$4.8 million	$8.1 million	$16.7 million
Compressors & Pumps	$1.2 million	$2.5 million	$4.0 million	$7.8 million
Electrical & Control Systems	$0.5 million	$1.0 million	$1.7 million	$3.2 million
Indirect Capital Costs	$1.5 million	$3.0 million	$4.5 million	$8.0 million
Total Capital Expenditure	$16.9 million	$32.9 million	$51.2 million	$94.4 million

The literature-sourced CAPEX rises from USD 16.9 million at 2 MTPD to USD 94.4 million at 18 MTPD. The increase is substantial in absolute terms, but the relevant economic question is the cost per unit of annual hydrogen output. Because utilisation increases the denominator of LCOH without increasing CAPEX proportionally, higher utilisation can produce a strong reduction in unit cost. The CAPEX values remain benchmark estimates rather than project quotations and should be replaced by vendor quotations and site-specific engineering estimates in a bankable study.

Annual OPEX increases with both plant capacity and utilisation in the supplied benchmark. These values are not recalculated from the technical simulation and therefore do not represent measured operating costs for the proposed HRS. Their role is to provide a transparent external cost basis for the discounted-cash-flow calculation. In a final project model, electricity, water, labour, maintenance, compressor replacement, storage inspection and insurance should be itemised separately.

Table 8
Literature-sourced annual OPEX benchmark.

Utilization Rate (%)	Operating Cost for 2 MTPD	Operating Cost for 4 MTPD	Operating Cost for 8 MTPD	Operating Cost for 18 MTPD
30%	$1.0 million	$2.0 million	$3.2 million	$6.1 million
50%	$1.2 million	$2.5 million	$4.0 million	$7.5 million
80%	$1.5 million	$3.0 million	$5.0 million	$9.3 million

LCOH is recalculated using a 20-year life, 8% discount rate, year-10 electrolyzer and battery replacements, 5% year-20 salvage value, and the annual hydrogen output implied by each capacity and utilization case. This replaces the previous simple division of total cost by lifetime hydrogen production.

At 80% utilisation, the recalculated LCOH decreases from 5.72 USD/kg H2 at 2 MTPD to 3.72 USD/kg H2 at 18 MTPD, a reduction of approximately 35.0%. This result is consistent with the existence of economies of scale in the assumed cost structure. It should not, however, be interpreted as evidence that an 18 MTPD station would necessarily achieve 3.72 USD/kg in a specific port, because electricity price, renewable resource, financing cost, storage pressure, grid interaction and actual demand can shift the result materially.

Table 9
Recalculated LCOH using explicit discounted-cash-flow assumptions.

System capacity	30% utilization	50% utilization	80% utilization
2 MTPD	$12.96/kg	$8.33/kg	$5.72/kg
4 MTPD	$12.74/kg	$8.33/kg	$5.63/kg
8 MTPD	$10.01/kg	$6.55/kg	$4.52/kg
18 MTPD	$8.30/kg	$5.41/kg	$3.72/kg

At 80% utilisation, the discounted payback is approximately 17 years for the 2 MTPD case at a hydrogen selling price of USD 6/kg and approximately 5 years at USD 10/kg. For the 18 MTPD case, the corresponding values are approximately 6 and 3 years. The wide spread demonstrates that payback is highly price-sensitive and should not be used as a standalone investment criterion. Net present value, internal rate of return, debt structure, tax treatment and downside scenarios would be required for a full investment appraisal.

Table 10
Discounted payback period at 80% utilisation under two hydrogen selling prices.

System capacity	Discounted payback at $6/kg	Discounted payback at $10/kg
2 MTPD	17 years	5 years
4 MTPD	17 years	5 years
8 MTPD	8 years	4 years
18 MTPD	6 years	3 years

Table 11
LCOH sensitivity for the 18 MTPD system to discount rate and utilisation.

Discount rate	30% utilization	50% utilization	80% utilization
6%	$7.27/kg	$4.79/kg	$3.34/kg
8%	$7.97/kg	$5.21/kg	$3.60/kg
10%	$8.72/kg	$5.66/kg	$3.88/kg

The principal interpretive result is that the corrected model changes the status of several conclusions in the original manuscript. The 180 h benchmark is adequate to diagnose short-term energy-flow behaviour, but it is not an adequate evidentiary basis for annual renewable-resource feasibility. Seven and a half days contain repeated diurnal cycles, yet they cannot represent seasonal solar geometry, seasonal wind regimes, prolonged low-resource events, annual maintenance, degradation or the statistical tails of weather variability. The correct inference is therefore conditional: the model demonstrates how the station responds to the supplied benchmark sequence, not how a real port would perform over an operating year.

Within that limitation, the short-horizon comparison is informative. Solar produces 246.86 kg H2 and wind 327.15 kg H2, so wind is 32.5% higher in cumulative production over the benchmark. Solar nevertheless reaches a 48.5% higher maximum electrolyser input. The distinction is operationally important because peak renewable power and cumulative fuel supply answer different design questions. A port operator may value continuity and inventory recovery more than peak electrolyser loading, while a designer may value high renewable peaks if storage and electrolyser capacity are available to absorb them. A defensible annual comparison must therefore include capacity factor, electrolyser utilisation, curtailment, storage cycling and unmet bunkering demand rather than a single production total.

The battery results further demonstrate the sensitivity of the station to temporal renewable structure. Under the corrected solar sequence, SOC declines from 50% to 20.32%, whereas under the wind sequence it increases to 89.64%. The difference is not evidence that one battery technology is inherently superior; it is a consequence of the supplied renewable-to-load profiles and the chosen initial condition. In an annual study, the relevant design metrics would include minimum SOC frequency, equivalent full

cycles, storage round-trip losses, hours at the SOC boundary and the probability that hydrogen demand cannot be met. These indicators should drive storage sizing rather than an arbitrary battery capacity selected independently of demand.

The station-level efficiency result is similarly conditional. The assumed PEM electricity consumption of 55.2 kWh/kg H2 corresponds to 60.4% LHV efficiency, while the addition of 2.0 kWh/kg for compression reduces the station-level value to approximately 58.3%. The numerical difference quantifies the importance of defining the system boundary. A future high-fidelity model should add water treatment, gas purification, cooling, compressor maps, pressure-dependent storage behaviour and auxiliary electricity because these loads can become material at station scale. The current values should therefore be regarded as transparent engineering benchmarks rather than as measurements.

The maritime demand interface changes the interpretation of production adequacy. A station that produces 32.91 or 43.62 kg/day on average over a short benchmark does not necessarily satisfy a vessel requiring a concentrated 50 kg bunkering event. Inventory and dispensing capacity must absorb the temporal mismatch. For this reason, HRS adequacy should be expressed in terms of service reliability: the probability of satisfying scheduled bunkering events, maximum waiting time, storage reserve, dispensing rate and unmet demand. The illustrative 25 kg/day demand used here is intentionally conservative and should be replaced by a mission-derived vessel profile before any operational conclusion is generalised.

The economic results provide a second-order insight into scale. At 80% utilisation, the calculated LCOH falls from 5.72 to 3.72 USD/kg H2 between 2 and 18 MTPD, a reduction of approximately 35%. This is a modelled scale effect, not a universal market relationship. The sensitivity analysis shows that utilisation and discount rate can move the calculated LCOH substantially; at 18 MTPD the reported screening range spans approximately 7.27 to 3.88 USD/kg across the tested utilisation and discount-rate combinations. The implication for maritime infrastructure is clear: securing reliable vessel offtake can be as important economically as increasing renewable capacity.

The literature benchmarks place these results in a plausible but demanding context. Recent Saudi optimisation studies report approximately 2.67–3.17 USD/kg H2 under favourable, location-specific assumptions, while a German HRS study reported 13.92–18.12 €/kg for a materially different demand and electricity-cost environment. The dispersion is not a contradiction; it demonstrates the sensitivity of LCOH to geography, electricity price, system boundary, demand resolution and financing assumptions. The present 3.72 USD/kg result should therefore be interpreted as an internally consistent screening output under stated assumptions rather than as a claim of market competitiveness.

The principal data limitation is provenance. The supplied manuscript does not contain the original irradiance and wind-speed records, turbine manufacturer curve, site coordinates or a validated vessel mission profile. The revised paper therefore removes the unsupported description of the series as real-time 2025 measurements. This is a substantive methodological correction rather than a cosmetic qualification. A publishable site-feasibility claim requires reproducible meteorological inputs, coordinate

metadata, data-quality procedures and a documented uncertainty treatment. Without these elements, resource-specific performance claims should remain explicitly conditional.

The principal model-fidelity limitation is also explicit. The revised framework captures the major energy and logistics interfaces but does not yet resolve detailed PEM polarisation behaviour, degradation, ramp-rate constraints, thermal management, water treatment, compressor performance maps, hydrogen purity dynamics or quantitative safety distances. These omissions do not invalidate the screening model, but they define the boundary of its validity. The appropriate next step is not to add unsupported numerical detail, but to replace engineering benchmarks with manufacturer or experimental data and then validate the model against measured operation.

Finally, the analysis does not demonstrate superiority of a hybrid solar-wind architecture. The contrasting benchmark trajectories provide a rational basis for testing a hybrid configuration because solar and wind exhibit different temporal patterns, but the combined system has not been simulated, optimised or validated in the present work. Any claim of hybrid superiority would therefore be speculative. The appropriate conclusion is that hybridisation is a testable design hypothesis whose value should be quantified in a subsequent annual optimisation using common site-specific meteorological data, vessel demand events and a traceable component-cost database.

Conclusion

This study has reformulated a renewable-powered maritime hydrogen refuelling concept as an integrated HRS comprising renewable electricity generation, a PEM electrolyser, battery storage, compression, high-pressure hydrogen storage and a vessel-demand interface. The correction of the original model materially changes the interpretation of the results. Over the 180 h benchmark, cumulative hydrogen production is 246.86 kg for solar and 327.15 kg for wind, corresponding to 32.91 and 43.62 kg/day on an arithmetic-average basis. Wind therefore produces 32.5% more cumulative hydrogen over this specific horizon, while solar reaches a 48.5% higher maximum electrolyser input of 222.06 kW compared with 149.49 kW for wind. The battery trajectories also diverge substantially: solar operation reduces SOC from 50% to 20.32%, whereas wind operation increases SOC to 89.64%.

Three conclusions follow for future research and design. First, the 180 h benchmark should be regarded only as a diagnostic short-horizon test; annual 8760 h, site-specific meteorological data are required to establish seasonal performance, renewable utilisation and hydrogen-supply reliability. Second, maritime adequacy must be evaluated against validated vessel mission and bunkering profiles, including storage inventory, dispensing rate, reserve margin and port operating windows. Third, hybrid solar-wind operation should remain a hypothesis until it is demonstrated through a common-site annual simulation and optimisation. The study therefore provides a reproducible methodological baseline rather than an investment-grade feasibility claim, and it identifies the specific data and model enhancements required to progress from screening analysis to engineering design and bankable techno-economic assessment.

The corrected energy metrics provide a more defensible basis for comparison. The PEM benchmark of 55.2 kWh/kg H2 corresponds to 60.4% LHV efficiency, while adding 2.0 kWh/kg for compression to 350 bar gives a station-level specific electricity requirement of 57.2 kWh/kg H2 and an LHV efficiency of approximately 58.3%. These values are engineering assumptions, not measurements. The techno-economic screening is likewise conditional: at 80% utilisation, calculated LCOH falls from 5.72 USD/kg H2 at 2 MTPD to 3.72 USD/kg H2 at 18 MTPD. The approximately 35% reduction illustrates the scale effect embedded in the adopted CAPEX/OPEX structure, while the sensitivity analysis demonstrates that utilisation, discount rate, selling price and replacement assumptions can materially alter the economic outcome.

Declarations

Ethics Declaration for Authors

7.1 Authorship and Contributor Statement

7.2 Originality and Plagiarism

7.3 Conflict of Interest

7.4 Funding Statement

Author Contribution

Authorship and contributor: all authors certify that all listed authors made significant intellectual contributions, and approve the final manuscript.□ Originality and plagiarism: all authors certify that the work is original, not been published anywhere.□ Conflict of interest: all authors certify that there are no financial or personal, academic relationships that could be perceived as biasing the research□ Funding statement: all authors certify that this research did not receive any funding from any source, and all authors collaborated to achieve these results independently without any funding.

References

1. International Energy Agency (IEA). (2025). *Global Hydrogen Review 2025*. IEA.
2. International Energy Agency (IEA). (2026). *Global Hydrogen Review 2026*. IEA.
3. International Maritime Organization (IMO). (2021). *Fourth IMO Greenhouse Gas Study 2020*. IMO.
4. International Maritime Organization (IMO). (2022). *MSC.1/Circ.1647*. Interim Guidelines for the Safety of Ships Using Fuel Cell Power Installations.
5. International Maritime Organization (IMO) (2023). 2023 IMO Strategy on Reduction of GHG Emissions from Ships. Resolution MEPC.377(80).

6. NASA POWER Project (2026). Prediction Of Worldwide Energy Resources (POWER): Hourly solar and meteorological data services.
7. Pompodakis, E. E., Orfanoudakis, G. I., Katsigiannis, Y. A., & Karapidakis, E. S. (2024). Hydrogen Production from Wave Power Farms to Refuel Hydrogen-Powered Ships in the Mediterranean Sea. *Hydrogen*, *5*(3), 494–518. https://doi.org/10.3390/hydrogen5030028
8. Qi, M., Vo, D. N., Yu, H., Shu, C. M., Cui, C., Liu, Y., Park, J., & Moon, I. (2023). Strategies for flexible operation of power-to-X processes coupled with renewables. *Renewable and Sustainable Energy Reviews*, *179*, 113282. https://doi.org/10.1016/j.rser.2023.113282
9. United Nations Conference on Trade and Development (UNCTAD) (2024). Review of Maritime Transport 2024. Geneva: United Nations.
10. Vazquez-Sanchez, H., Okeke, I. J., Singh, E., Baaqel, H., Saville, B. A., MacLean, H. L., & Sarathy, S. M. (2025). A life cycle assessment of e-hydrogen production using proton-exchange membrane water electrolysis coupled with desalination in Saudi Arabia. *International Journal of Hydrogen Energy*, *139*, 792–805. https://doi.org/10.1016/j.ijhydene.2025.05.154
11. Wang, Z., Li, M., Zhao, F., Zhao, F., Ji, Y., & Han, F. (2024). Status and prospects in technical standards of hydrogen-powered ships for advancing maritime zero-carbon transformation. *International Journal of Hydrogen Energy*, *62*, 925–946. https://doi.org/10.1016/j.ijhydene.2024.03.083
12. Wolf, N., Neuber, R., Mädlow, A., & Höck, M. (2025). Techno-economic analysis of green hydrogen supply for a hydrogen refueling station in Germany. *International Journal of Hydrogen Energy*, *106*, 318–333. https://doi.org/10.1016/j.ijhydene.2025.01.424
13. Zhaka, V., & Samuelsson, B. (2024). Hydrogen as fuel in the maritime sector: From production to propulsion. *Energy Reports*, *12*, 5249–5267. https://doi.org/10.1016/j.egyr.2024.11.005
14. Al Baity, O. A., Ahmed, Y. M., Abdelnaby, M., & ElGohary, M. M. (2025). Green Fuels for Maritime: An Overview of Research Advancements, Applications, and Challenges. *Marine Technology Society Journal*, *59*(1), 132–146. https://doi.org/10.4031/MTSJ.58.4.3
15. Al-Enazi, A., Okonkwo, E. C., Bicer, Y., & Al-Ansari, T. (2021). A review of cleaner alternative fuels for maritime transportation. *Energy Reports*, *7*, 1962–1985. https://doi.org/10.1016/j.egyr.2021.03.036
16. Ammar, N. R., & Alshammari, N. F. S. H. (2018). Overview of the Green Hydrogen Applications in Marine Power Plants Onboard Ships. *International Journal of Multidisciplinary and Current Research*, *6*(01). https://doi.org/10.14741/ijmcr.v6i01.10912
17. Brynolf, S., Baldi, F., & Johnson, H. (2016). Energy Efficiency and Fuel Changes to Reduce Environmental Impacts. *Shipping and the Environment* (pp. 295–339). Springer. https://doi.org/10.1007/978-3-662-49045-7_10
18. Dall'Armi, C., Pivetta, D., & Taccani, R. (2023). Hybrid PEM Fuel Cell Power Plants Fuelled by Hydrogen for Improving Sustainability in Shipping: State of the Art and Review on Active Projects. *Energies*, *16*(4), 2022. https://doi.org/10.3390/en16042022
19. Davis, N. N., Badger, J., Hahmann, A. N., Hansen, B. O., Mortensen, N. G., Kelly, M., Larsén, X. G., Olsen, B. T., Floors, R., Lizcano, G., Casso, P., Lacave, O., Bosch, A., Bauwens, I., Knight, O. J., van

Potter, A., Fox, R., Parvanyan, T., Hansen, K., & Drummond, S. B., R (2023). The Global Wind Atlas: A High-Resolution Dataset of Climatologies and Associated Web-Based Application. *Bulletin of the American Meteorological Society*, *104*(8), E1507–E1525. https://doi.org/10.1175/BAMS-D-21-0075.1

20. Elkafas, A. G., & Seddiek, I. S. (2024). Application of renewable energy systems in seaports towards sustainability and decarbonization: Energy, environmental and economic assessment. *Renewable Energy*, *228*, 120690. https://doi.org/10.1016/J.RENENE.2024.120690
21. Elkafas, A. G., & Shouman, M. R. (2022). A Study of the Performance of Ship Diesel-Electric Propulsion Systems From an Environmental, Energy Efficiency, and Economic Perspective. *Marine Technology Society Journal*, *56*(1), 52–58. https://doi.org/10.4031/MTSJ.56.1.3
22. Fu, Z., Lu, L., Zhang, C., Xu, Q., Zhang, X., Gao, Z., & Li, J. (2023). Fuel cell and hydrogen in maritime application: A review on aspects of technology, cost and regulations. *Sustainable Energy Technologies and Assessments*, *57*, 103181. https://doi.org/10.1016/j.seta.2023.103181
23. Guan, W., Chen, L., Wang, Z., Chen, J., Ye, Q., & Fan, H. (2024). A 500 kW hydrogen fuel cell-powered vessel: From concept to sailing. *International Journal of Hydrogen Energy*, *89*, 1466–1481. https://doi.org/10.1016/J.IJHYDENE.2024.09.418
24. Jimenez, V. J., Kim, H., & Munim, Z. H. (2022). A review of ship energy efficiency research and directions towards emission reduction in the maritime industry. *Journal of Cleaner Production*, *366*, 132888. https://doi.org/10.1016/j.jclepro.2022.132888
25. Kolodziejski, M. (2024). Review of hydrogen-based propulsion systems in the maritime sector. *Archives of Thermodynamics*, 335–380. https://doi.org/10.24425/ather.2023.149728
26. Laurence, A., Wright, & Yifan Wang. (2021). A Comparative Review of Alternative Fuels for the Maritime Sector: Economic, Technology, and Policy Challenges for Clean Energy Implementation. *World*, *2*(4), 456–481.
27. Mallouppas, G., Yfantis, E., & Ar (2021). Decarbonization in Shipping Industry: A Review of Research, Technology Development, and Innovation Proposals. *Journal of Marine Science and Engineering*, *9*(4), 415. https://doi.org/10.3390/jmse9040415
28. Nuchturee, C., Li, T., & Xia, H. (2020). Energy efficiency of integrated electric propulsion for ships – A review. *Renewable and Sustainable Energy Reviews*, *134*, 110145. https://doi.org/10.1016/j.rser.2020.110145
29. Di Micco, S., Mastropasqua, L., Cigolotti, V., Minutillo, M., & Brouwer, J. (2022). A framework for the replacement analysis of a hydrogen-based polymer electrolyte membrane fuel cell technology on board ships: A step towards decarbonization in the maritime sector. *Energy Conversion and Management*, *267*(115893).
30. Sadek, I., & Elgohary, M. (2020). Assessment of renewable energy supply for green ports with a case study. *Environmental Science and Pollution Research*, *27*(5), 5547–5558. https://doi.org/10.1007/S11356-019-07150-2
31. Seddiek, I. S., & Ammar, N. R. (2023). Carbon footprint and cost analysis of renewable hydrogen-fuelled ships. *Ships and Offshore Structures*, *18*(7), 960–969.

https://doi.org/10.1080/17445302.2022.2093031

32. Shakeri, N., Zadeh, M., & Bremnes Nielsen, J. (2020). Hydrogen Fuel Cells for Ship Electric Propulsion: Moving Toward Greener Ships. *IEEE Electrification Magazine*, *8*(2), 27–43. https://doi.org/10.1109/MELE.2020.2985484
33. Sürer, M. G., & Arat, H. T. (2022). Advancements and current technologies on hydrogen fuel cell applications for marine vehicles. *International Journal of Hydrogen Energy*, *47*(45), 19865–19875. https://doi.org/10.1016/j.ijhydene.2021.12.251
34. Temiz, M., & Dincer, I. (2021). Techno-economic analysis of green hydrogen ferries with a floating photovoltaic based marine fueling station. *Energy Conversion and Management*, *247*, 114760. https://doi.org/10.1016/j.enconman.2021.114760
35. Tomislav, B., & Juraj Bukša. (2024). Hydrogen as a Viable Energy Source in Maritime Coastal Transport. *Journal of Maritime & Transportation Sciences*, *64*(1), 9–30.
36. Ustolin, F., Campari, A., & Taccani, R. (2022). An Extensive Review of Liquid Hydrogen in Transportation with Focus on the Maritime Sector. *Journal of Marine Science and Engineering*, *10*(9), 1222. https://doi.org/10.3390/jmse10091222
37. Van Hoecke, L., Laffineur, L., Campe, R., Perreault, P., Verbruggen, S. W., & Lenaerts, S. (2021). Challenges in the use of hydrogen for maritime applications. *Energy & Environmental Science*, *14*(2), 815–843. https://doi.org/10.1039/D0EE01545H
38. Wang, Z., Li, M., Zhao, F., Ji, Y., & Han, F. (2024). Status and prospects in technical standards of hydrogen-powered ships for advancing maritime zero-carbon transformation. *International Journal of Hydrogen Energy*, *62*, 925–946. https://doi.org/10.1016/j.ijhydene.2024.03.083
39. Mandal, A., Singha, H., & Mohapatra, P. (2024). *Development of roadmap for a green hydrogen cluster in Ramagundam*. Deutsche Gesellschaft für Internationale Zusammenarbeit (GIZ) GmbH.
40. Wei, D., Zhang, L., Alotaibi, A. A., Fang, J., & Alshahri, A. H. (2022). Transient simulation and comparative assessment of a hydrogen production and storage system with solar and wind energy using TRNSYS. International Journal of Hydrogen Energy. Retrieved from https://www.sciencedirect.com/science/article/pii/S0360319922007716
41. Li, R., Jin, X., Yang, P., Sun, X., Zhu, G., & Zheng, Y. (2023). Techno-economic analysis of a wind-photovoltaic-electrolysis-battery hybrid energy system for power and hydrogen generation. Energy Conversion and Management. Retrieved from https://www.sciencedirect.com/science/article/pii/S0196890423002005
42. Akhavan Shams, S., & Ahmadi, R. (2021). Dynamic optimization of solar–wind hybrid system connected to electrical battery or hydrogen as an energy storage system. *International Journal of Energy Research*, *45*(12), 17351–17370. https://doi.org/10.1002/er.6549
43. Al-Sharafi, A., Sahin, A. Z., Ayar, T., & Yilbas, B. S. (2017). Techno-economic analysis and optimization of solar and wind energy systems for power generation and hydrogen production in Saudi Arabia. Renewable and Sustainable Energy Reviews, 69, 33–45. Retrieved from https://www.sciencedirect.com/science/article/pii/S136403211630908X

44. Nasser, M., Megahed, T. F., & Ookawara, S. (2022). A review of water electrolysis–based systems for hydrogen production using hybrid/solar/wind energy systems. Environmental Science and Pollution Research, 29(27), 40621–40643. Retrieved from https://link.springer.com/article/10.1007/s11356-022-23323-y
45. Herdem, M. S., Mazzeo, D., Matera, N., & Baglivo, C. (2024). A brief overview of solar and wind-based green hydrogen production systems: Trends and standardization. International Journal of Hydrogen Energy. Retrieved from https://www.sciencedirect.com/science/article/pii/S0360319923024904
46. Benghanem, M., Mellit, A., Almohamadi, H., & Haddad, S. (2023). Hydrogen production methods based on solar and wind energy: A review. Energies, 16(2), 757. Retrieved from https://www.mdpi.com/1996-1073/16/2/757
47. Acakpovi, A., Adjei, P., & Nwulu, N. (2020). Optimal hybrid renewable energy system: A comparative study of wind/hydrogen/fuel-cell and wind/battery storage. Journal of Renewable Energy, 2020, Article 1756503. https://doi.org/10.1155/2020/1756503
48. Lazaroiu, G., Osman, M. G., & Strejoiu, C. V. (2023). Performance evaluation of renewable energy systems: Photovoltaic, wind turbine, battery bank, and hydrogen storage. Batteries, 9(9), 468. Retrieved from https://www.mdpi.com/2313-0105/9/9/468
49. Shaner, M. R., Atwater, H. A., & Lewis, N. S. (2016). A comparative technoeconomic analysis of renewable hydrogen production using solar energy. Energy & Environmental Science, 9(7), 2354–2371. Retrieved from https://pubs.rsc.org/en/content/articlehtml/2016/ee/c5ee02573g

Figures

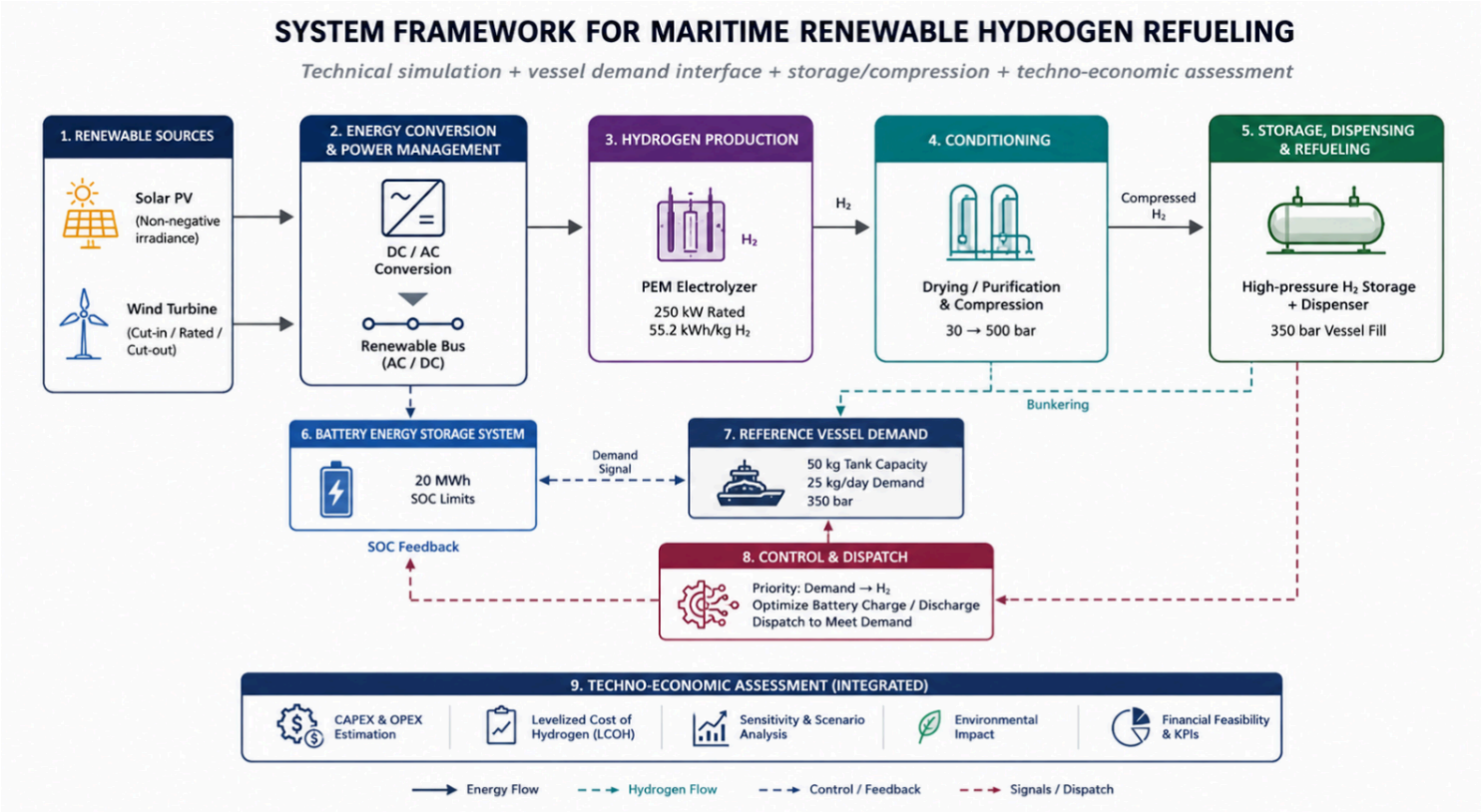


Figure 1

Revised integrated framework for renewable hydrogen production, storage, compression, and maritime refueling.

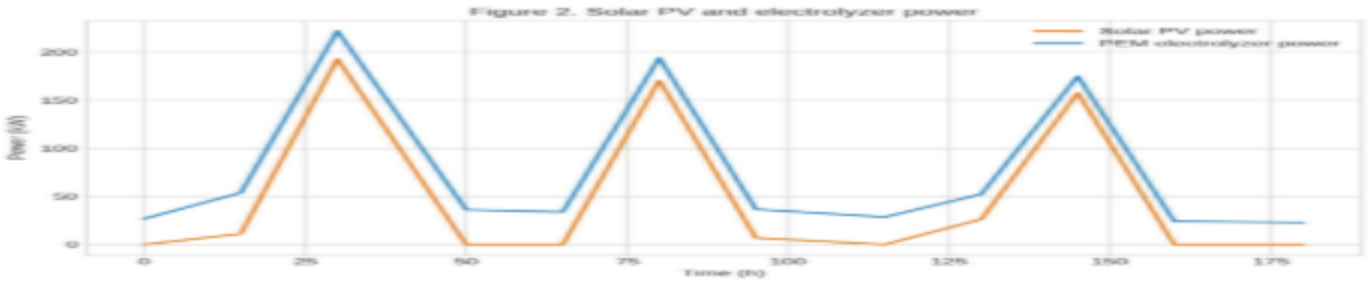


Figure 2

Solar PV and PEM electrolyzer power over the 180 h benchmark.

Shows that electrolyzer power follows the benchmark solar profile but can exceed instantaneous PV output because the battery supplies the difference. The maximum electrolyzer power is 222.06 kW at 30 h.

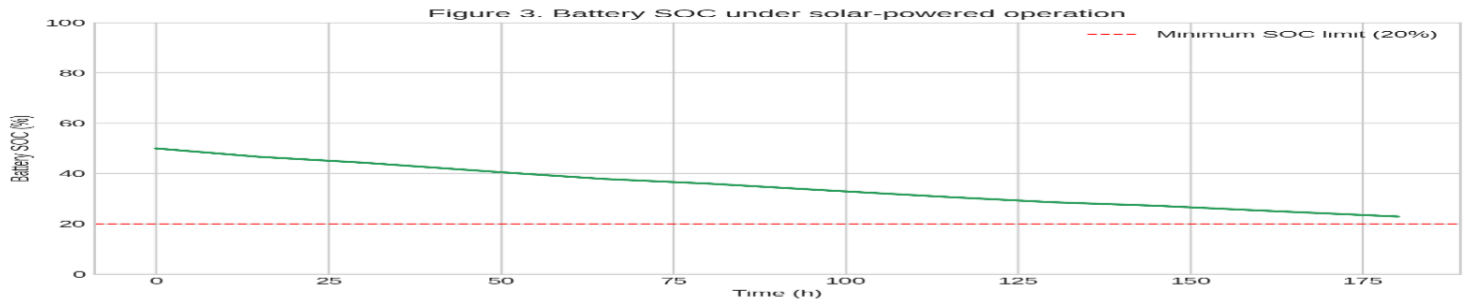


Figure 3

Battery SOC under solar-powered operation.

Shows the corrected battery SOC trajectory. The battery starts at 50%, declines to 20.32%, and does not reach the lower limit within the 180 h benchmark. The monotonic decline reflects the absence of large renewable surplus intervals in the supplied solar

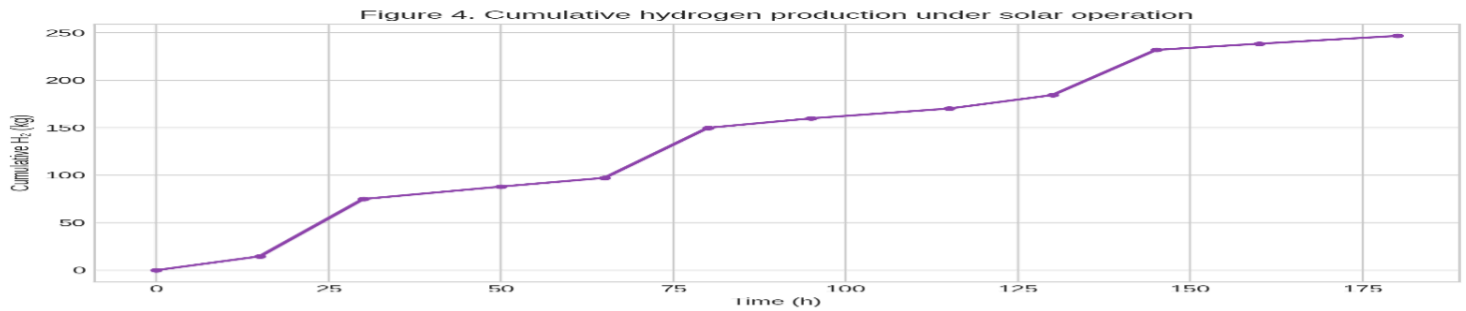


Figure 4

Cumulative hydrogen production under solar operation.

Reports cumulative hydrogen rather than a production rate. The cumulative curve reaches 246.86 kg at 180 h. The instantaneous production rate is obtained separately from $\dot{m}H2$ = PEL/55.2 and is therefore expressed in kg/h.

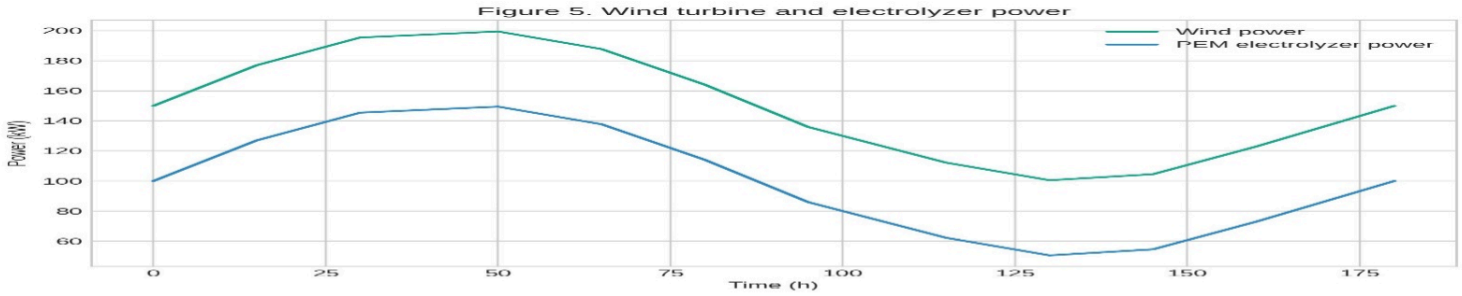


Figure 5

Wind turbine and PEM electrolyzer power over the 180 h benchmark.

Illustrates the relatively continuous wind input and the lower peak electrolyzer power compared with the solar case. The maximum electrolyzer power is 149.49 kW at 50 h.



Figure 6

Battery SOC under wind-powered operation.

Shows the corrected wind battery behavior. The battery SOC increases from 50% to 89.64% because renewable power exceeds the combined electrolyzer and compression loads. This is physically consistent with the stated charging convention.

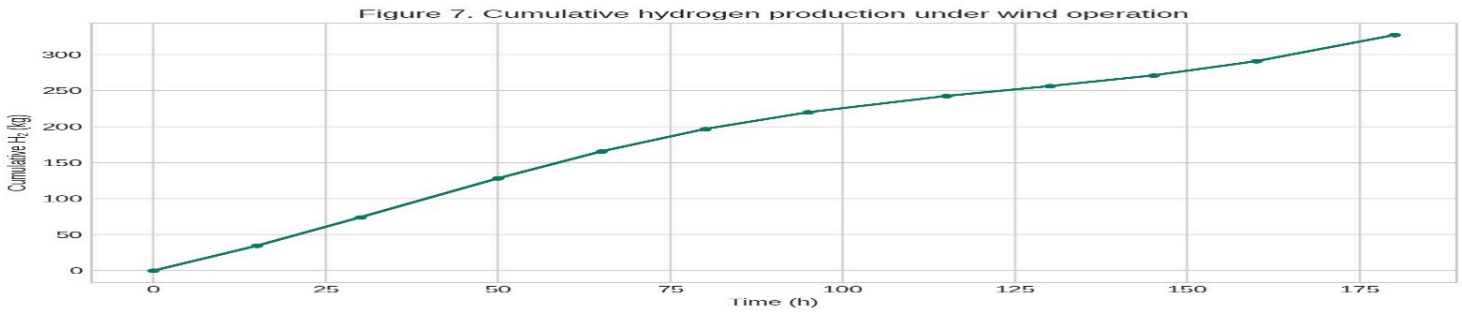


Figure 7

Cumulative hydrogen production under wind operation.

Reports cumulative hydrogen starting from zero. The cumulative production reaches 327.15 kg at 180 h. The original 50 kg hydrogen inventory at hour zero was removed because it represented an unexplained initial production value rather than cumulative output.

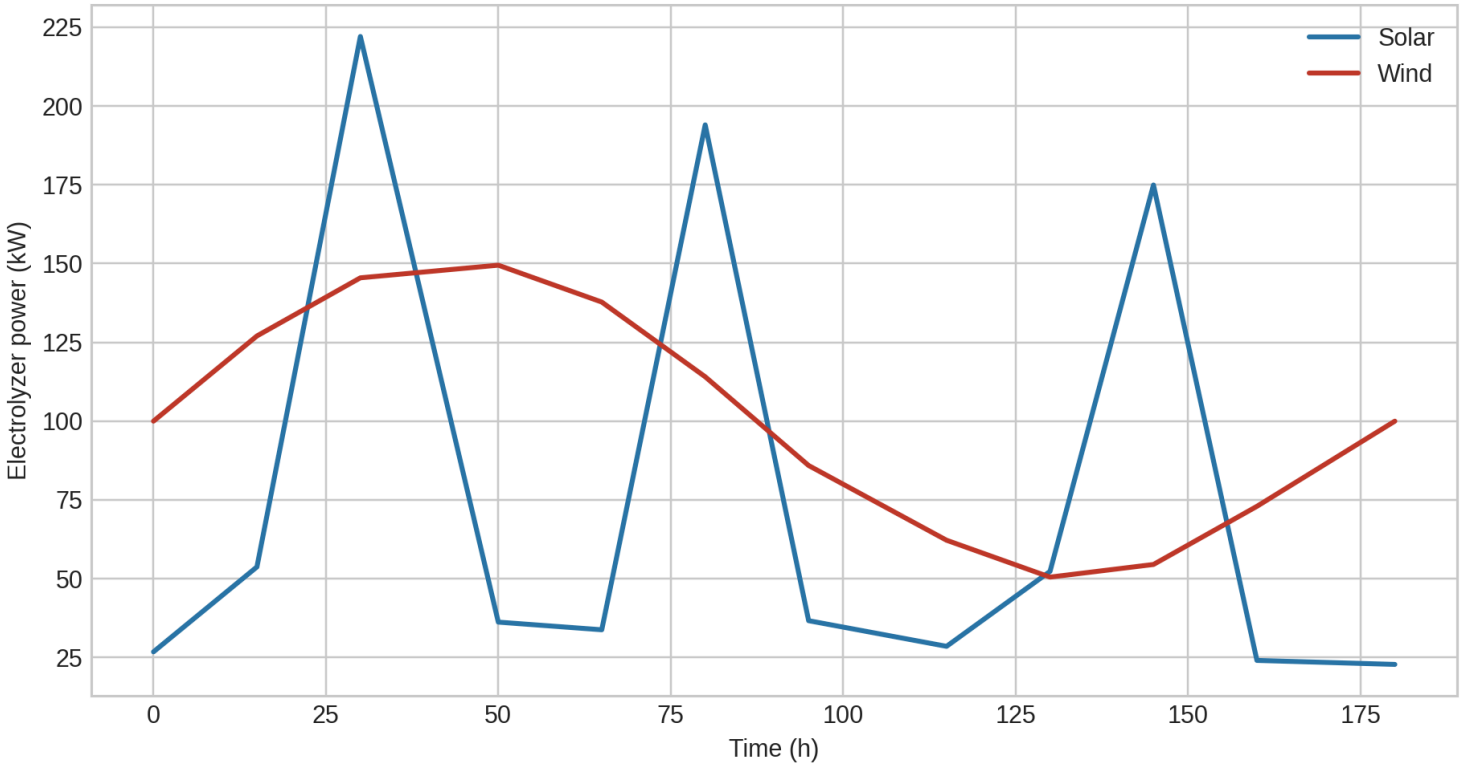


Figure 8

Solar versus wind electrolyzer power.

Confirms that solar provides the higher instantaneous electrolyzer power, whereas wind provides a lower but more continuous operating profile. The maximum values are 222.06 kW for solar and 149.49 kW for wind.

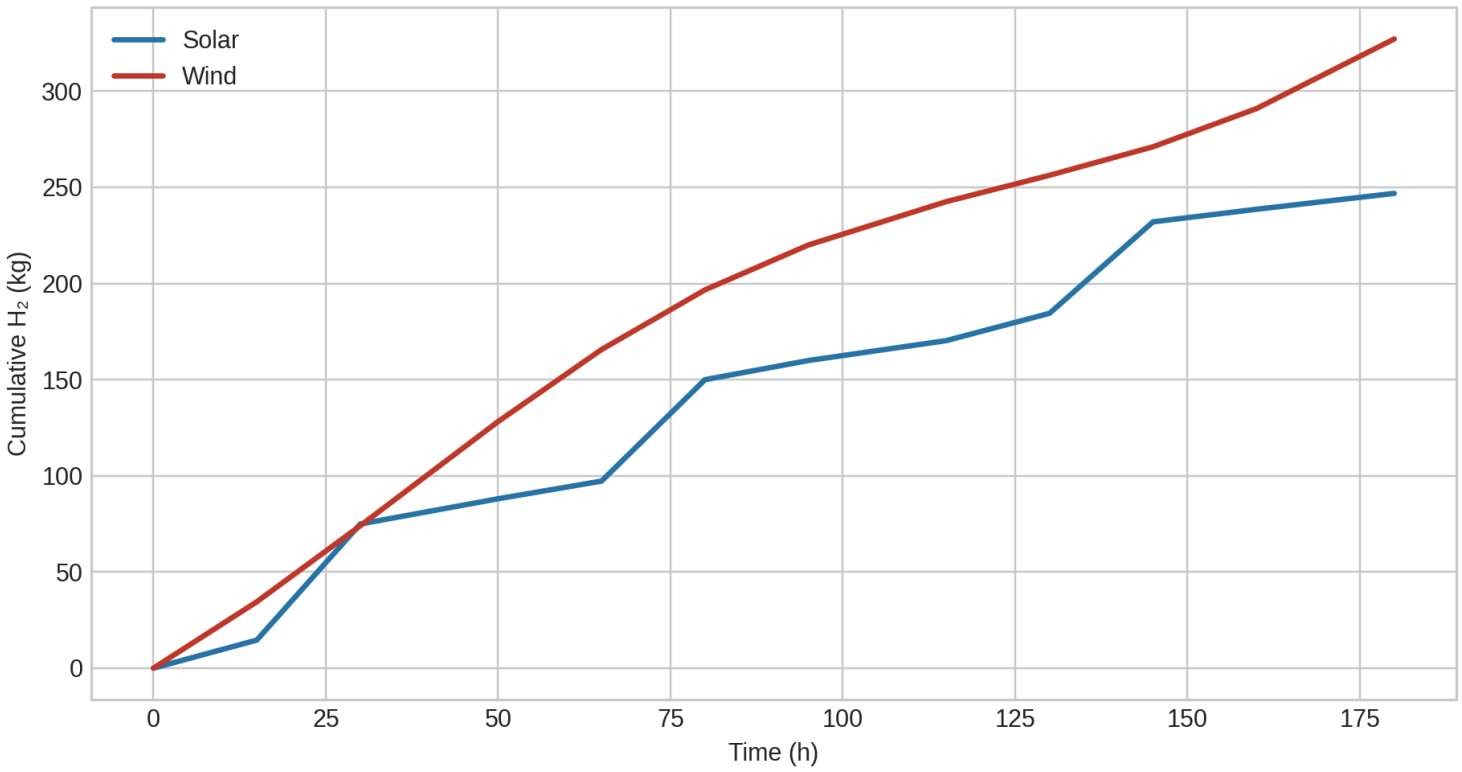


Figure 9

Solar versus wind cumulative hydrogen production.

Shows cumulative hydrogen production. Wind reaches 327.15 kg by 180 h compared with 246.86 kg for solar. The difference is primarily attributable to the continuous wind input in the benchmark rather than to a demonstrated superiority of wind at a real port location.

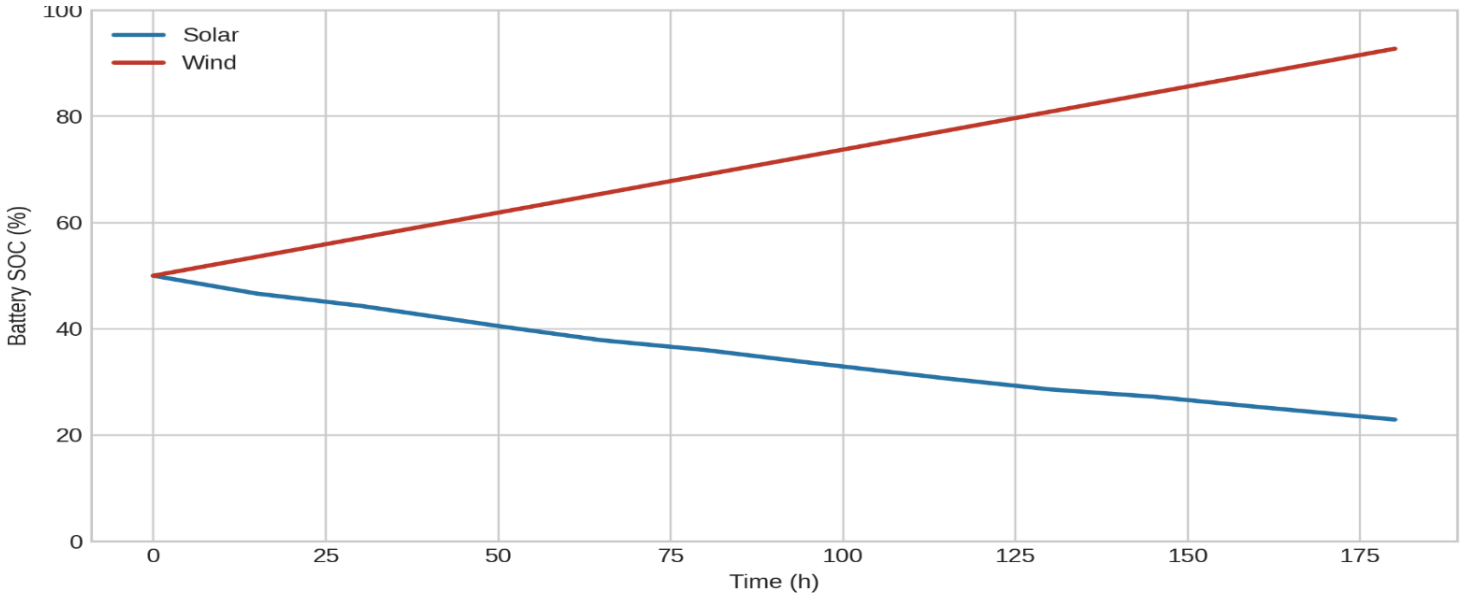


Figure 10

Solar versus wind battery SOC.

Shows the physically consistent SOC trajectories. Solar declines toward its 20% lower operating limit, while wind charges toward 90%. The difference reflects the renewable-to-load balance in the supplied benchmark series and the 20 MWh battery assumption.

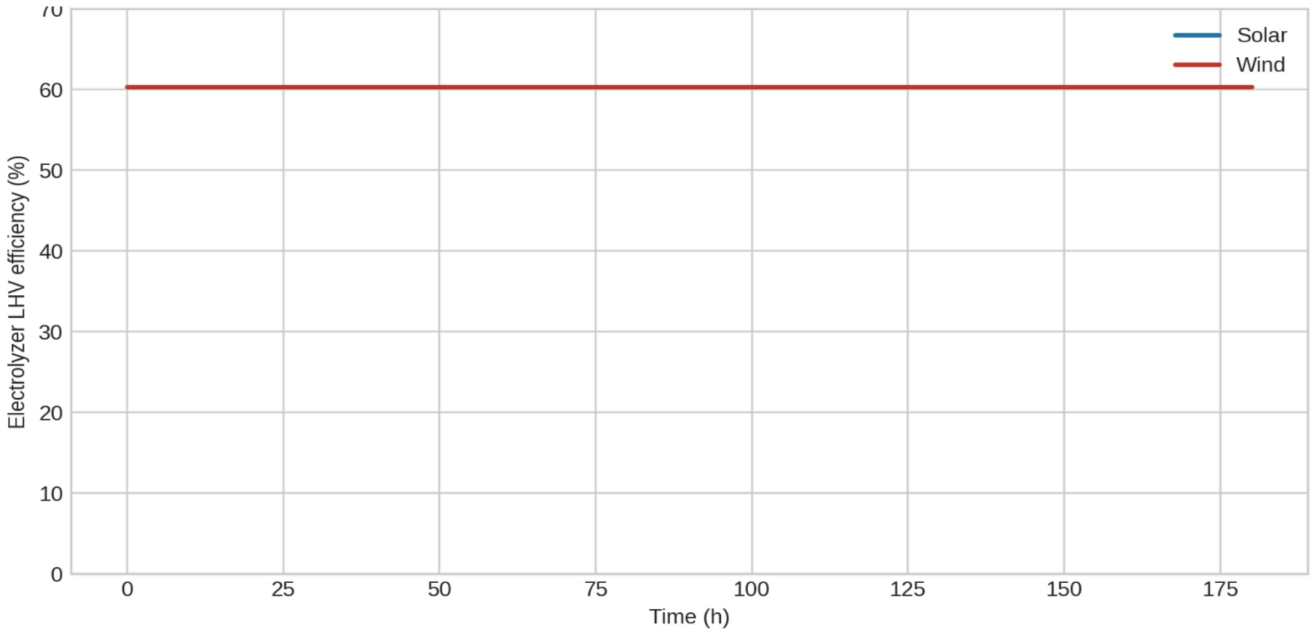


Figure 11

Presents dimensionally valid energy efficiencies. The electrolyzer-level LHV efficiency is 60.4%, while the station-level value including compression is 58.3%. These are screening assumptions based on the stated specific-energy values, not time-varying measured efficiencies.

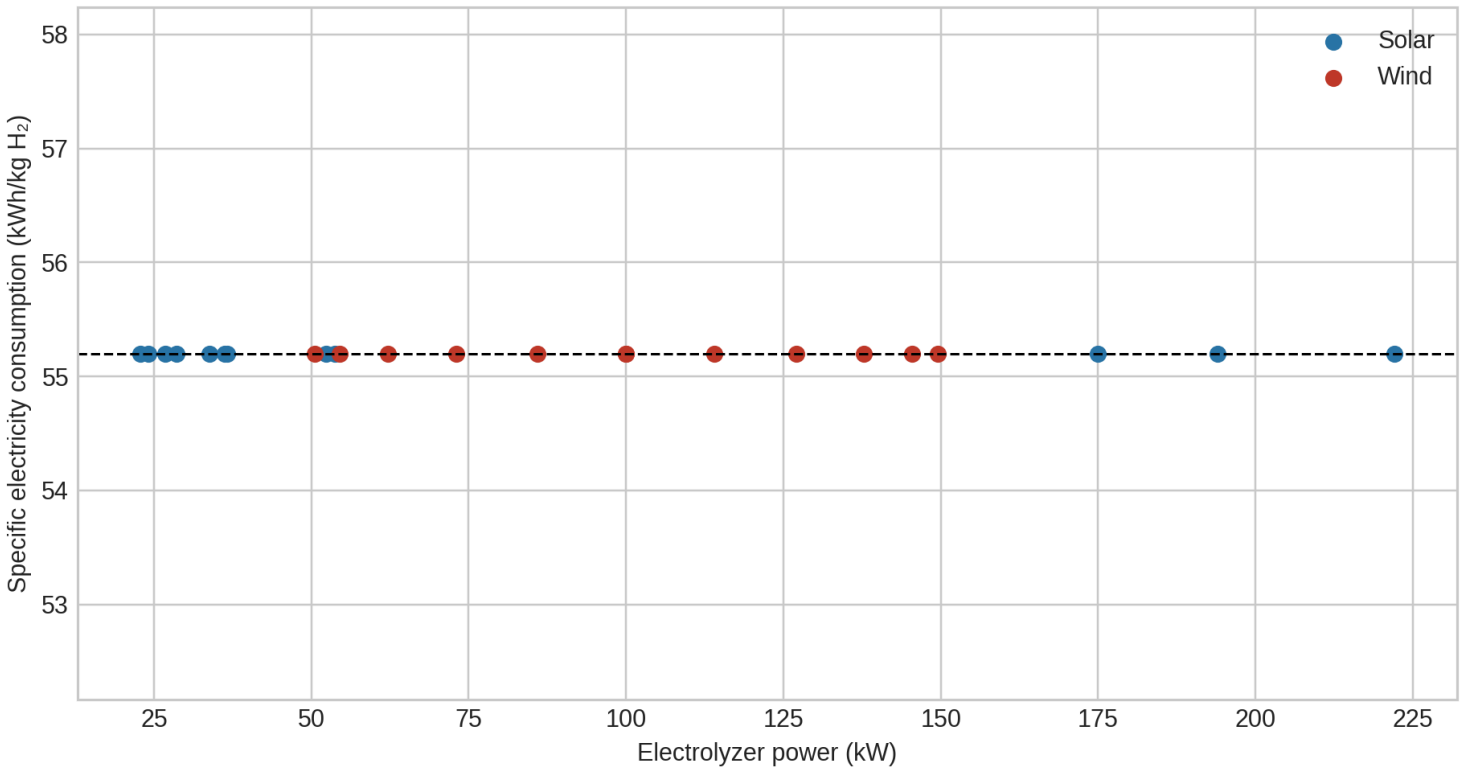


Figure 12

Reports specific electricity consumption rather than the previous dimensionally incorrect metric. The electrolyzer benchmark is 55.2 kWh/kg H2 and the station-level value including compression is 57.2 kWh/kg H2.